Enhanced electron confinement in pyramidal nanostructures

C. Tournier-Colletta, B. Kierren, Y. Fagot-Revurat, C. Chatelain, and D. Malterre*
Institut Jean Lamour, UMR 7198, Nancy-Université - B.P. 239 F-54506 Vandœuvre-lès-Nancy, France
(Received 5 July 2011; revised manuscript received 29 July 2011; published 11 October 2011)

From scanning tunneling spectroscopy measurements, we recently found evidence for the effect of electron-phonon interactions on the lifetime of hot electrons and holes. This information was obtained by measuring the linewidth of quantum well states resulting from the confinement of Shockley states in truncated hexagonal Ag nanopyramids. In the present paper, we show that a careful analysis allows us to obtain both the intrinsic and extrinsic broadening contributions. This latter contribution results from the lossy boundary scattering which is strongly reduced in this peculiar geometry. Indeed, we deduce the energy dependence of the reflection coefficient which remains higher, as usually observed in nanostructures like adatom islands and quantum corrals.

DOI: 10.1103/PhysRevB.84.165420 PACS number(s): 73.20.At, 61.46.Hk, 68.37.Ef, 72.10.Di

I. INTRODUCTION

In a recent publication,[1] we presented evidence for the effect of electron-phonon coupling on the lifetime of electron states in Ag. This was achieved by exploiting confined states in Ag nanostructures on a Ag(111) film with a special geometry (truncated hexagonal pyramids). In such nanostructures, the Shockley state is confined to the top layer and exhibits narrow resonant modes depending on the lateral size of the pyramid. The electron lifetime was obtained by measuring the differential conductance with a scanning tunneling microscope (STM) at low temperature. This spectroscopic technique, called scanning tunneling spectroscopy (STS), allows us to obtain conductance spectra at a given point or spectroscopic map at a given energy which, in a simple approach, can be identified with the spatial distribution of the local density of states. Other techniques like photoemission and two-photon photoemission have also been used in recent years to determine the spectral linewidth and lifetime of surface states.[2,3] The knowledge of the electron lifetime is important because it gives the coherence length which plays a fundamental role for the electronic properties; in particular, transport. From a theoretical point of view, the lifetime concept is related to the notion of a quasiparticle developed to describe low-energy excitations in ordinary metals. Due to many-body interaction between electrons, an elementary excitation corresponding to an additional electron or a hole is not an independent entity. It is a quasiparticle with an effective mass that depends on the strength of the interaction and with a well-defined momentum, but an energy only defined within an uncertainty ΔE[4] that is related to the lifetime by $\Delta E\tau \sim \hbar$. In the Fermi liquid model, which is valid for most three-dimensional metals, the lifetime diverges for zero-energy excitations.

Different STS-derived methods can be used to probe either the coherence length or the linewidth of excitations; both being related to electron lifetime. On the one hand, the coherence length can be obtained from the damping of the quantum interference patterns due to the scattering of the surface state by a step edge or a quantum corral.[5,6] On the other hand, the linewidth can be directly obtained by measuring the differential conductivity spectra (dI/dV) at a fixed point above the surface. But as this spectroscopic technique is not selective in momentum, it is limited not only to discrete states like confined states in nanostructures (e.g., adatom islands on a surface or artificial quantum corrals[7–9]), but also to the discontinuity in the density of states like the onset of the surface Shockley state.[10]

However, in nanostructures, an additional mechanism leads to a supplementary broadening of the linewidth of confined states. This is related to the partial confinement resulting from the boundary potential of the nanostructure being not infinite. This lossy boundary scattering originates from the transmission of the Shockley state through the boundary potential but also from the absorption of the Shockley state due to scattering into the bulk states. Following the optics analogy proposed by Avouris *et al.*,[11] the imperfect confinement can be simply described by a reflection coefficient. The energy dependence of this coefficient has been determined with high accuracy for Ag(111) step edges.[12] The lossy boundary scattering broadening, which depends on the reflection coefficient,[13] increases with increasing deviation from total reflection ($R = -1$). Unfortunately, in many cases, the reflection coefficient is small,[14] leading to a broadening contribution which dominates the intrinsic contributions. This is a severe limitation for the determination of the electron lifetime; in particular, close to the Fermi surface where the lifetime (linewidth) is large (small). Nevertheless, our recent investigation of the linewidth of Shockley states confined in truncated hexagonal Ag pyramids provides evidence of the effect of electron-phonon coupling on the electron lifetime:[1] the low-energy excitations exhibit the characteristic signature of this coupling; that is, a sudden decrease of the linewidth in an energy range corresponding to the Debye frequency at the Fermi energy. This was achieved thanks to the exploitation of the spatial dependence of the confined states and, to a lesser extent, to the fact that the lossy broadening is reduced in such a geometry.

The present paper focuses on the lossy boundary scattering broadening by a careful analysis of the linewidth of confined Shockley states in truncated hexagonal Ag pyramids from low-temperature STS measurements. By exploiting the different symmetries of the resonant modes and their spatial distributions, we determine the linewidths of about 15 confined states. We demonstrate that the lossy boundary broadening is smaller than the broadening usually observed in quantum corrals or adatom islands. From the energy dependence of this contribution, we deduce the reflection coefficient and show that it is significantly reduced with respect to the standard value.

II. EXPERIMENTAL DETAILS

The measurements were carried out in an ultrahigh vacuum (UHV) setup composed of a molecular beam epitaxy chamber for the elaboration and characterization of the surfaces, a scanning tunneling microscopy (STM) chamber equipped with a 5 K Omicron STM, and a photoemission chamber with a high resolution Scienta SES 200 analyzer. The Cu(111) single crystal was cleaned by several cycles of Ar^+ etching and annealing at 500 °C and it was characterized by STM and Auger electron spectroscopy (AES). Ag adatoms were evaporated from a Knudsen cell at the rate of 1 ML/min to obtain a film about 15 monolayers (MLs) thick. The surface state parameters (effective mass and energy) are known from photoemission measurements to be progressively modified from the substrate values to the Ag(111) values.[15,16] For film thicknesses larger than 15 MLs, the surface-state values of Ag(111) are restored. The dI/dV maps (and spectra) were recorded at 5 K in the open feedback loop mode using the lock-in technique with a bias modulation in the range of 1 to 3 meV rms at 700 Hz. For 1 meV rms, the instrumental resolution (about 3.5 meV) leads to a negligible broadening of less than 1 meV for the narrowest spectral feature. High-frequency voltage noise could increase the instrumental broadening but we think that such a mechanism is negligible. The additional broadening we observe depends on the measured nano-object in the same sample and is interpreted as resulting from the defect contribution.

To compare with spectroscopic maps, we considered numerically the problem of an electron confined in an hexagonal well with infinite potential. The first stationary states, and the associated energies, have been computed by means of a Lanczos-type diagonalization of the Hamiltonian.

III. EXPERIMENTAL RESULTS AND DISCUSSION

A. Probing different symmetries

Growth mode of epitaxial Ag films on Cu(111) single crystal allows the formation of three-dimensional nanostructures. Indeed, at low deposition temperature, one observes Ag truncated pyramids corresponding to the stacking of 4 to 6 atomic layers on relatively thick (about 10 to 15 ML) Ag film.[1] The lateral size distribution is quite large and many of them have a nearly hexagonal symmetry. Figure 1(a) shows an STM image of such a pyramid. The corner-corner distance in the hexagonal top layer is 17 nm. Figure 1(b) reports a spectroscopic image corresponding to the dI/dV map recorded at $U = 0.27$ mV. The bright signal represents the maxima of the standing-wave pattern associated with the Shockley surface state at this energy. It reveals the lateral confinement of the Shockley surface state in the nanostructured surface. Figure 1(c) presents a series of spectroscopic images at different energies corresponding to resonant modes of the hexagonal nanopyramids. Close to the minimum of the surface band, the fundamental mode (at −41 meV) consists of a broad lobe centered in the hexagon. With increasing energy, we observe excited modes with hexagonal symmetry. As expected, the number of nodes increases with energy, and we point out that some of them are characterized by zero intensity at the center. This reflects the symmetry (C_{6v} group) of the hexagonal potential and, more precisely, the symmetry of the different modes. An eigenstate must have the symmetry of one of the irreducible representations of the group, but only one representation (the fully symmetric A_1 representation) exhibits nonzero weight at the center. The determination of the different modes has been previously reported in hexagonal adatom islands by Li *et al.*[7,17] and we will show below how the spatial distribution of these modes can be exploited to obtain their energy and spectral linewidth. Such measurements were systematically achieved as illustrated in Fig. 2. For example, we report in Fig. 2(b) a dI/dV map as a function of energy and position along the high-symmetry direction of the hexagonal face corresponding to the white lines in the STM image [Fig. 2(a)]. This spectral map, corresponding to the density of states in one direction, exhibits the different modes, their spatial localization (horizontal axis), and their energy width (vertical axis). Two spectra recorded at two different points (♯1 and ♯2 in the STM image) and corresponding to the two dashed white lines in the spectroscopic map are reported in Fig. 2(c). These spectra are fit by a sum of Lorentzian functions, convoluted by the narrow experimental resolution, whose positions determine the confined state energies and widths and their total linewidth. A very good agreement between experimental and fitted curves (solid lines) is obtained. By changing the tip position, the energy and linewidth of the spectral features remain unchanged, only their intensity, which is proportional to the square of the confined wave function, is modified. At point ♯1, corresponding to the center of the nanostructure, only resonant modes having A_1 symmetry can be probed (for example, the 10th mode which is close to

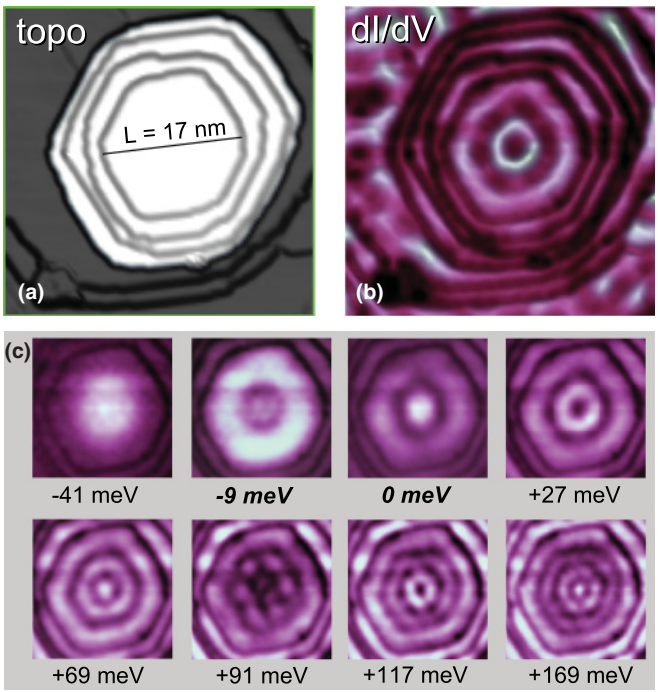

FIG. 1. (Color online) (a) Topographic STM image of a truncated hexagonal Ag pyramid ($U = -0.3$ V, $I = 1$ nÅ). (b) Spectroscopic image (dI/dV) recorded at $U = 27$ mV. (c) Series of spectroscopic images recorded at several energies showing different quantum well states of the resonator.

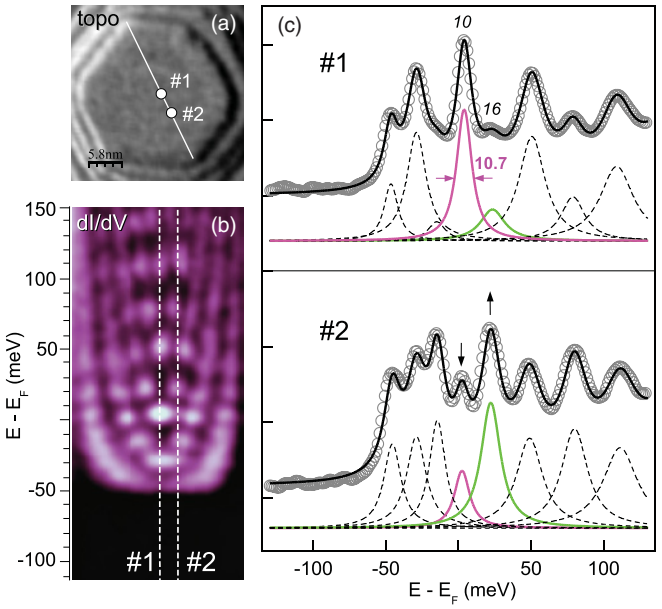

FIG. 2. (Color online) (a) Topographic image of 25 nm pyramid indicating the two points ♯1 and ♯2 corresponding to the STS spectra shown in (c). (b) Spectroscopic map obtained from 64 dI/dV spectra recorded along the line in the topographic image. (c) STS spectra (dI/dV) recorded at points ♯1 and ♯2. The solid black line represents the fitting curve composed of Lorentzian structures (dashed lines) associated with the confined states. The pink (∼0 meV) and green (∼30 meV) lines represent the spectral signatures of modes 10 and 16.

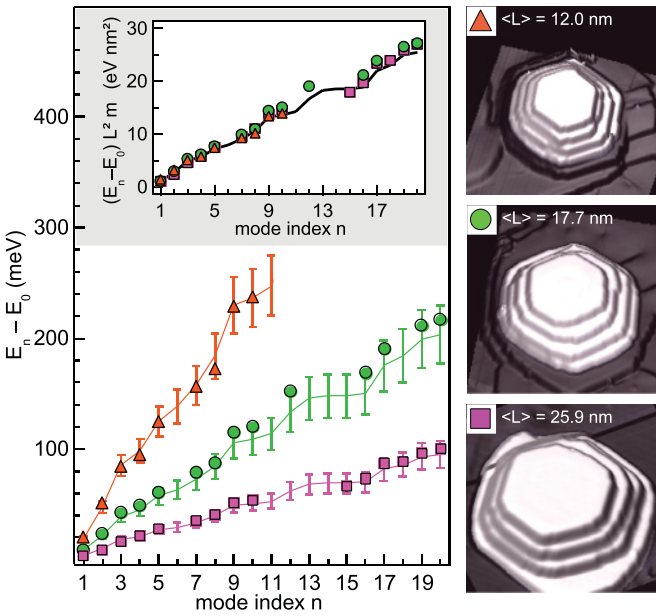

FIG. 3. (Color online) Comparison between experimental energies (symbols) for the different resonant modes with energies calculated in a simple infinite quantum well resonator (lines) for the three pyramids represented in the right part of the figure. The top curve shows that the experimental energies follow a scaling behavior, as expected from the theoretical model.

the Fermi energy). By moving the tip position from point ♯1 to point ♯2, the intensity of the structures having A_1 symmetry decreases whereas the structures corresponding to other irreducible representations increase. This symmetry sensitivity is illustrated by the evolution of the 10th and 16th structures, which exhibit opposite evolution. We would like to point out that the 16th structure, which should have a zero intensity at the center, has a small finite intensity. This is due to the spatial resolution of the tip. The energy and linewidth of the different modes can be obtained with accuracy at the tip position where the structure is intense. This method allows us to determine the energy and linewidth of the first confined states. This is in contrast with many lifetime studies in the literature, which usually only focus on spectra at the nanostructure center.[7,9]

B. Energy of resonator modes

In Fig. 3 we compare quantum well state energies corresponding to three pyramid sizes (12.0, 17.7 and 25.9 nm) with energies (ε_n) calculated in the framework of a two-dimensional hexagonal infinite potential (n is the mode index). The experimental energies are taken relative to the Shockley band onset E_0 (kinetic energies). In these truncated pyramids, it was found at $E_0 = -50$ meV; a value which is slightly higher than the corresponding Shockley energy for the Ag(111) single crystal (−65 meV). The error bars for the calculated values are due to the uncertainty of electron effective mass and pyramid size. The size parameter $\langle L \rangle$ is obtained from an average over the different corner-corner distances measured by STM. A very good agreement is obtained. Some modes (for example the 6th and 11th modes) cannot be probed because their spectral intensities are too small in the recorded direction. As expected from confinement effects, the smaller the pyramids, the higher the energies since the confined state energy for an infinite potential varies with the size L of the hexagon according to:[7]

$$\varepsilon_n = \frac{\mu_n}{m^* L^2}, \tag{1}$$

where μ_n is a number characterizing the mode index and m^* is the effective mass of the Shockley state ($m^* = 0.4 \pm 0.02 m_0$). The scaling behavior of the energy as a function of pyramid size is illustrated in the top curve where we have reported the experimental energy $E_n - E_0$ times the effective mass and the square of the pyramid length. The agreement corroborates the fact that an infinite hexagonal well is a satisfactory model, at least for the 20 first states.

A more stringent argument is the comparison of the two-dimensional spectroscopic map at a given energy with the calculated electron density of the corresponding mode. However, we have to take into account the finite linewidth of the experimental peaks. As shown in Fig. 2(c), this linewidth increases with increasing energy (the origin of this behavior will be discussed later). Therefore, at a given bias voltage, the STS map probes several modes close in energy. As a consequence, a spectroscopic map cannot be compared directly with a single-mode-calculated electron density. The neighboring modes should slightly contribute to the experimental intensity. In Fig. 4, we compare the fourth ("4"), seventh ("7"), and tenth ("10") experimental modes with the calculated electron density ($|\Psi|^2$). To take into account the finite linewidth, $|\Psi|^2$ is a mixture of several hexagonal-well-calculated electron densities $|\Phi_n|^2$. For example, for the fourth experimental map,

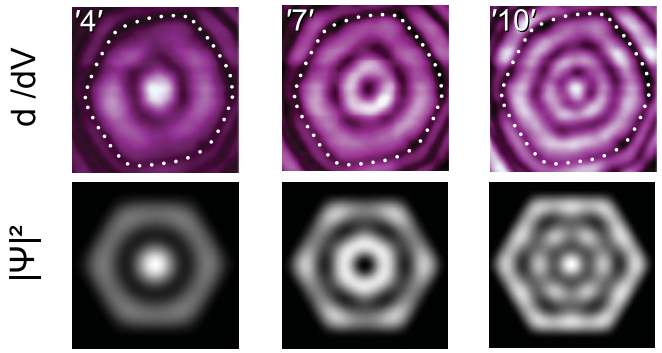

FIG. 4. (Color online) Spectroscopic image (top) and calculated electron density (bottom) associated with the "4," "7," and "10" modes of the hexagonal resonator.

one has

$$|\Psi_4|^2 \propto |\Phi_4|^2 + 0.15\,(|\Phi_3|^2 + |\Phi_5|^2 + |\Phi_6|^2),$$

where the 0.15 coefficient has been empirically found for the best agreement with experiments. Because with increasing energy the linewidth increases and the energy separation between two adjacent modes decreases, the contributions of the neighboring modes are more important. For the tenth mode, we have

$$|\Psi_{10}|^2 \propto |\Phi_{10}|^2 + 0.6(|\Phi_9|^2 + |\Phi_{11}|^2).$$

In conclusion, the simple model of an infinite hexagonal quantum well provides a satisfactory description of the energy of the resonances as well as their spatial distributions in the top layer of the nanopyramids.

C. Linewidth: intrinsic and extrinsic lifetime

Now we would like to discuss the spectral width and then the lifetime of the electron excitations. As discussed in the introduction, there are several contributions to the linewidth: intrinsic contributions reflecting the lifetime of electron excitations in solids and extrinsic contributions resulting from the fact that the measured states are confined in a nanostructure with particular boundary conditions. The intrinsic linewidth depends on the different interactions in the solid. In noble metals, it is composed of mainly three contributions associated with electron-electron ($\Gamma_{e\text{-}e}$), electron-phonon interactions ($\Gamma_{e\text{-ph}}$), and interactions with defects (Γ_{def}). As demonstrated by Landau,[4] the low-energy electron-electron excitations lead to a linear shift of the energy associated with the real part of the self-energy [$\Delta E = \alpha(E - E_F)$] and a quadratic energy dependence of $\Gamma_{e\text{-}e}$ [$\Gamma_{e\text{-}e} = \beta(E - E_F)^2$] reflecting the self-energy imaginary part. However, the energy and broadening contributions are vanishing at the Fermi energy (E_F) so that, very close to E_F, the electron-phonon contribution ($\Gamma_{e\text{-ph}}$) is the dominant mechanism. In the simple Debye phonon model,[18] it is given by

$$\Gamma_{e\text{-ph}} = 2\pi \int \alpha^2 F(\omega)[1 + 2n(\omega) + f(E + \omega) - f(E - \omega)]d\omega,$$

where $n(\omega)$ and $f(\omega)$ are, respectively, the Bose-Einstein and the Fermi functions. The Eliasberg coupling function $\alpha^2 F(\omega)$ is equal in a system characterized by the Debye frequency ω_D up to $\lambda(\omega/\omega_D)^2$, where λ is a free dimension parameter characterizing the electron-phonon coupling. Finally, the last contribution (Γ_{def}) due to the scattering of electrons by defects can be considered to be energy independent. The electron-phonon contribution depends on a characteristic energy scale, which is the Debye energy in this simple model. At low temperature with respect to the Debye temperature, the energy dependence of the electron-phonon linewidth exhibits a pronounced increase close to ω_D and a plateau at higher energy. The value of the plateau is proportional to the electron-phonon coupling (λ).[19] This dependence is illustrated by the dashed line in the inset of Fig. 5 with $\lambda = 0.09$, $\omega_D = 20$ meV, and $T = 5$ K. Such values yield a plateau $\Gamma^{\text{sat}}_{e\text{-ph}} = 4$ meV. These parameters have to be considered as effective parameters which reproduce the dependence measured by photoemission on flat Ag(111).[20] The extrinsic contribution results from the fact that the measured states are confined in a nanostructure and that there is an additional broadening associated with the lossy boundary scattering. Indeed, this mechanism can be understood by the partial confinement of the Shockley state in the nanostructure since, at the nanostructure boundary, the electronic waves can be scattered into the bulk state (absorption) or transmitted in the surface state outside the top layer. As mentioned in the introduction, this extrinsic contribution is usually the dominant mechanism and prevents the precise determination of the intrinsic linewidth.[21] However, a scattering model has been developed to quantify this lossy boundary scattering.[13] For a circular resonator of diameter L, the linewidth of the nth confined state with energy E_n is given by

$$\Gamma_R(E_n) = -\frac{2\hbar^2}{m^*}\sqrt{\frac{2m^* E_n}{\hbar^2}}\frac{\ln|R(E_n)|}{L}, \qquad (2)$$

where $R(E_n)$ is the reflection coefficient at energy E_n and m^* is the effective mass of the electron. This equation shows that, for a fully reflective wall corresponding to $R = -1$ (infinite potential limit), $\Gamma_R(E_n) = 0$ since, in this limit, there is no transmission and no absorption of the electronic waves and the surface states are perfectly confined in the nanostructure. However, one is generally far from this ideal situation. The energy dependence of the reflection coefficient $R(E)$ has been measured from the damping of the standing waves, which develop close to a monoatomic step (ascending and descending) on the surface.[12] This experimental determination shows that $|R|$ is much smaller than unity. This is corroborated by theoretical calculations which yield values around 0.3 to 0.4 in most cases.[14] This step-reflection coefficient has been used to model this extrinsic contribution in nanostructures like monoatomic islands or vacancy islands on a surface.[21,22] The typical energy dependence of Γ_R is depicted in the dotted-dashed line in the inset of Fig. 5. The sum of the electron-phonon and lossy scattering contributions represented by the pink solid line in the same inset exhibits two singular points indicated by arrows. The first one, at the onset of the surface state and then zero kinetic energy, corresponds to a zero-Γ_R contribution whereas the second one, just at the Fermi level, corresponds to a zero–electron-phonon contribution. These two minima in the linewidth are clearly seen in the experimental linewidth measured in two pyramids (17 and

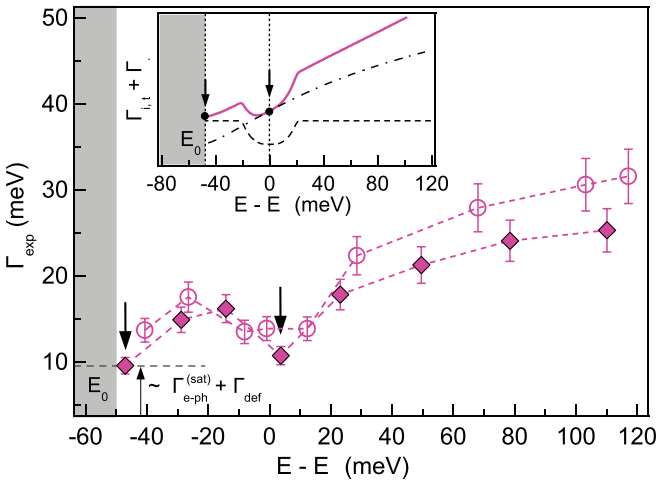

FIG. 5. (Color online) Experimental spectral linewidth as a function of energy for the confined states in two different pyramid sizes (circles 17 nm and diamonds 25 nm). The black dashed horizontal line represents the maximum electron-phonon and defect contributions. The two arrows represent the position of the two minima at the bottom of the Shockley band and at the Fermi energy. Inset gives the schematic shape of the electron-phonon contribution (dashed line) and the lossy scattering mechanism (dotted-dashed line) The pink solid line is the sum of these two contributions.

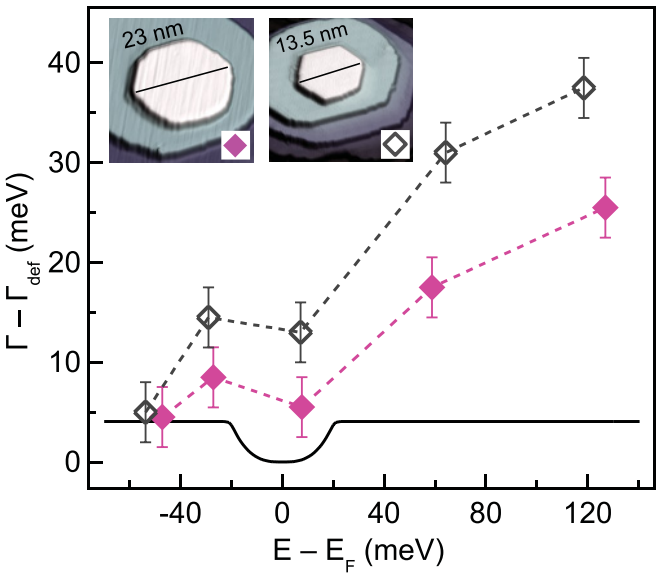

FIG. 6. (Color online) Experimental spectral linewidth as a function of energy for the confined states in two different monoatomic islands (open is 13.5 nm and filled is 23 nm). The solid line represents the intrinsic linewidth due to electron-phonon coupling.

25 nm). Therefore, the raw data clearly provide evidence of a dip at E_F extending over the energy range from -20 to $+20$ meV, which is in qualitative agreement with the Debye energy of Ag. Moreover, the dependence at high energy is dominated by the Γ_R contribution. Quantitative information can be obtained by exploiting these two particular points. The linewidth at the onset of the Shockley band is simply the sum of the defect contribution and the electron-phonon broadening, which is the plateau value $\Gamma^{\rm sat}_{e\text{-ph}}$. The electron-electron interaction could yield an additional broadening. However, at this energy very close to the Fermi level, its contribution to the linewidth is smaller than 0.5 meV. This value can be estimated from the theoretical calculation which shows that intraband decay is the dominating mechanism.[22–24] An adjustment of this calculation by a quadratic energy dependence leads to $\beta = 2.7 \times 10^{-4}$ meV^{-1}, in qualitative agreement with previous photoemission data.[20] Such a dependence ignores the deviation from the Landau asymptotic behavior evidenced recently.[22] However, in the explored energy range ($E - E_F < 140$ meV), the electron-electron broadening remains small (smaller than 5 meV at 140 meV).

Therefore, from the linewidth at the bottom of the Shockley band, it is possible to determine the defect contribution which is found to be about 6.5 meV. The second particular value at the Fermi energy is simply $\Gamma_R(E_F) + \Gamma_{\rm def}$, hence $\Gamma_R(E_F) = 4$ meV. In order to extract the intrinsic contribution, a quantitative description of the lossy boundary scattering is needed over the whole energy range; in other words, it is necessary to determine the appropriate reflection coefficient which appears in Eq. (2).

Let us first consider the standard case of adatom islands corresponding to a well-known reflection coefficient. In Fig. 6, we present the linewidth measured in two adatom hexagonal islands (13.5 and 23 nm) found on terraces of the same Ag film on Cu(111). The defect contribution has been subtracted by using the method presented above. Close to the Fermi energy a dip reveals the electron-phonon coupling, like in nanopyramids, but it seems to be less pronounced because of a larger Γ_R contribution. The lossy broadening, which is zero at the bottom of the Shockley band, remains weak up to the Fermi energy as shown in the STS spectrum of Fig. 7(a), which was recorded from the center of an hexagonal $L = 17$ nm adatom island and which exhibits two structures with very narrow spectral width: 7.5 meV for the structure close to the bottom of the band and 8.5 meV for the structure close to the Fermi energy. The boundaries of such islands consist of monoatomic steps and it has been demonstrated that the reflection coefficient determined experimentally from the damping of the standing waves close to a linear step edge[5] (called step coefficient in the following) can be used to model the reflection-broadening contribution in Ag islands on Ag.[13,21] The energy dependence of this step-reflection coefficient is reproduced in the inset of Fig. 7(b): $|R|$ decreases from 1 at the bottom of the Shockley band to about 0.4 for 250-meV-kinetic-energy electrons. With such a dependence, the broadening at E_F remains less than 6 meV, as shown in the inset of Fig. 7(a). This means that the defect contribution is about 2 to 3 meV in this island and confirms that $\Gamma_{e\text{-ph}} \approx 4$ meV in agreement with calculations and photoemission experiments.[20]

We have extracted the reflection broadening contribution in these adatom islands by removing from the experimental linewidth all intrinsic contributions; that is, electron-electron, electron-phonon, and defect broadening contributions: $\Gamma_{\rm expt}(E) - \Gamma_{e\text{-}e}(E) - \Gamma_{e\text{-ph}}(E) - \Gamma_{\rm def}$. The electron-electron and electron-phonon contributions have been calculated as explained above and the defect contribution can been estimated by exploiting the linewidth of the fundamental mode close

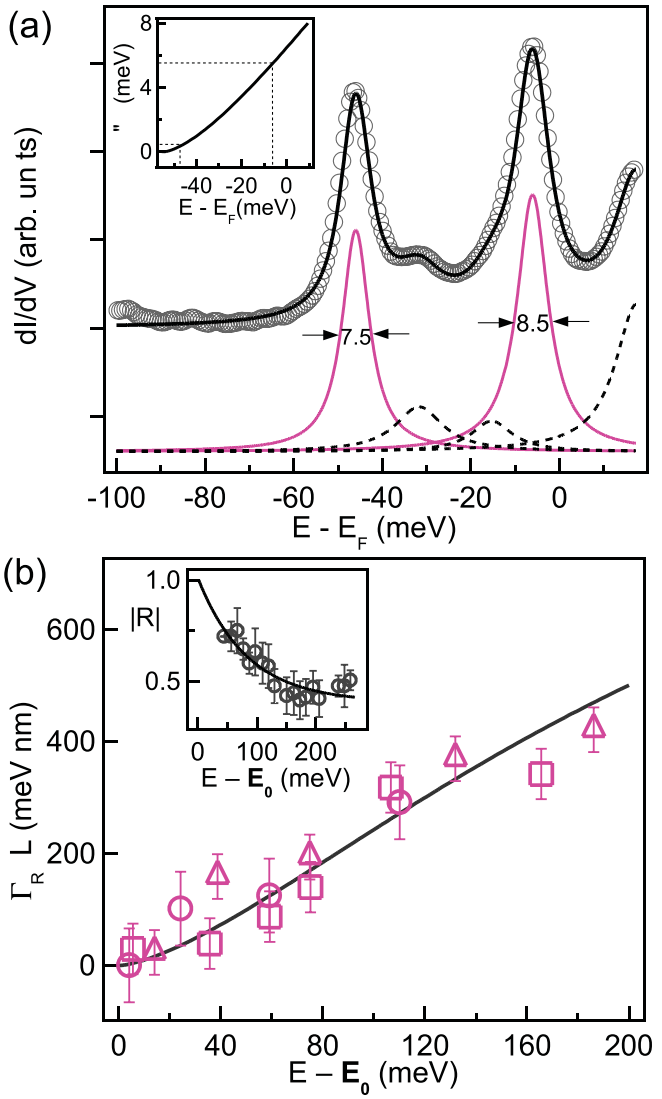

FIG. 7. (Color online) (a) Experimental spectrum recorded from the center of an adatom island ($L = 17$ nm). Dashed and solid (pink) lines are Lorentzian curves associated with resonant-mode signatures. The inset presents the lossy scattering broadening (Γ_R) calculated from the energy-dependent reflection coefficient determined in.[5] (b) Comparison between the size-rescaled calculated (solid line) and experimental (symbols) lossy scattering broadening for 3 different island sizes ($\Gamma_R L$). The inset shows the step-reflection coefficient.[5]

to the Shockley band bottom. Since the lossy scattering broadening in principle obeys a scaling behavior in which it scales with the island size, as revealed by Eq. (2), we have reported in Fig. 7(b) the experimental extrinsic broadening for three different island sizes (13.5, 17, and 23 nm) renormalized by their size and compared them with the product $\Gamma_R L$ calculated with Eq. (2). As the lossy scattering broadening has to vanish at the band bottom E_0, the value has been reported as a function of the kinetic energy $E - E_0$. A very good agreement between experimental and calculated values for the three pyramids is obtained, confirming the validity of the step-reflection coefficient for such adatom islands.

The same analysis can be carried out for nanopyramids. We report in Fig. 8(a) the experimental linewidth of the states confined in a 17.7 nm pyramid (the constant defect contribution estimated to be 9.2 meV has been removed). We compare the experimental data with a calculated dependence taking into account the same electron-electron, electron-phonon, and lossy scattering broadening contributions (dashed line) as in the previous case (adatom islands). The latter contribution has been calculated by using the step-reflection coefficient which nicely fits the linewidth in adatom islands. This comparison shows that the calculated values reproduce the experimental linewidths at low energies (for $E < 40$ meV) but significantly deviate at higher energies, indicating that the genuine reflection coefficient $|R|$ is larger than the step-coefficient in the high-energy range. Therefore, we adapt the energy dependence of the reflection coefficient in order to reproduce the experimental data. This procedure leads to the reflection coefficient described by the solid line in the inset of Fig. 8(a). $|R|$ remains around 0.7 for 200 meV kinetic energy, in contrast to its rapid decrease for monoatomic steps and adatom islands. Such a high reflection coefficient has been observed recently at stacking-fault-induced fractional steps on Ag(111)

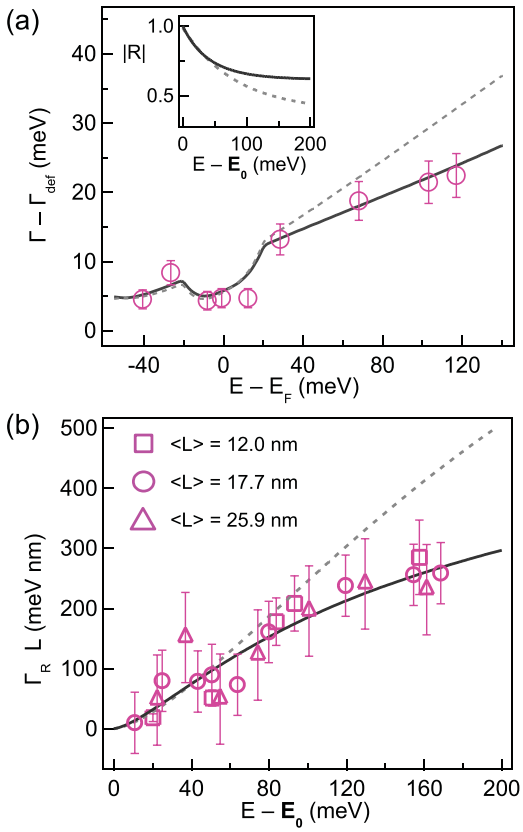

FIG. 8. (Color online) (a) Defect-free linewidths of states confined in a 17 nm pyramid (the defect contribution has been subtracted from the raw experimental linewidth). The dashed and solid lines represent the sum of the electron-phonon and lossy scattering contributions, respectively, calculated with the two reflection coefficients illustrated in the inset. (b) Size-scaled lossy scattering contribution for three different pyramid sizes (symbols) and contribution calculated with the reflection coefficient illustrated by the solid line of inset of (a).

surfaces.[25] The lossy scattering broadening calculated with this high reflection coefficient [solid line in Fig. 8(a)] is found to be in very good agreement with experimental extrinsic linewidth obtained by subtracting the intrinsic contribution from the experimental linewidth for several pyramids. In this figure, we have exploited the scaling behavior by reporting $\Gamma_R L$ as a function of the kinetic energy in Fig. 8(b). The agreement between experimental and calculated values demonstrate that the same reflection coefficient can be used whatever the nanopyramid size.

This analysis shows that the reflection coefficient in nanopyramids is larger than the step-reflection coefficient observed in adatom islands. This strongly suggests that absorption and transmission probabilities, which are respectively associated with scattering from the confined surface state to bulk states and to the surface state outside the top layer of the nanostructure, are reduced in this pyramidal geometry. It is clear that monoatomic step edges are far from ideal reflectors for electrons because leakage occurs into the surface state on the other side and into the bulk state of the crystal.[5,14] The geometry of the nanopyramid favors a higher reflection coefficient. First, the height of the pyramids (4 to 5 atomic layers) likely yields a decrease of the transmission into the surface state of the underlying layer. Second, it seems intuitive that the the decay mechanism of the surface state into the bulk is also reduced because of the lower overlapping of the surface state with bulk states in the nanopyramid.

IV. CONCLUSION

In conclusion, we have performed 5 K STS measurements on truncated Ag hexagonal nanopyramids. We showed that the confined-state energy can be simply described in the framework of an infinite potential quantum well model. We also showed that the spectral linewidth of confined states close to the Fermi energy provides evidence of the signature of electron-phonon coupling. Moreover, the linewidth remains narrow at relatively high energy in contrast to the results obtained in quantum corrals and adatom islands. This reflects a more efficient confinement of the Shockley state (i.e., a higher reflection coefficient) due to the peculiar geometry of these pyramidal nanostructures which reduces transmission and absorption processes. We develop a method to extract the intrinsic contribution from which we propose an energy-dependent reflection coefficient for the Shockley state in these nanopyramids.

*dani6el.malterre@ijl.nancy-universite.fr

[1] C. Tournier-Colletta, B. Kierren, Y. Fagot-Revurat, and D. Malterre, Phys. Rev. Lett. **104**, 016802 (2010).
[2] P. M. Echenique, R. Berndt, E. V. Chulkov, Th. Fauster, A. Goldmann, and U. Höfer, Surf. Science Rep. **52**, 219 (2004).
[3] R. Matzdorf, Surf. Science Rep. **30**, 153 (1998); Chem. Phys. **151**, 151 (2000).
[4] D. Pines and Ph. Nozières, *the Theory of Quantum Liquids* (Benjamin, New York, 1969).
[5] L. Bürgi, O. Jeandupeux, H. Brune, and K. Kern, Phys. Rev. Lett. **82**, 4516 (1999).
[6] K.-F. Braun and K.-H. Rieder, Phys. Rev. Lett. **88**, 096801 (2002).
[7] J. Li, W. D. Schneider, R. Berndt, and S. Crampin, Phys. Rev. Lett. **80**, 3332 (1998).
[8] J. Kliewer, R. Berndt, and S. Crampin, New J. Phys. **3**, 22 (2001).
[9] H. Jensen, J. Kröger, R. Berndt, and S. Crampin, Phys. Rev. B **71**, 155417 (2005).
[10] J. Li, W.-D. Schneider, R. Berndt, O. R. Bryant, and S. Crampin, Phys. Rev. Lett. **81**, 4464 (1998).
[11] Ph. Avouris, I.-W. Lyo, R. E. Walkup, and Y. Hasegawa, J. Vac. Sci. Technol. B **12**, 1447 (1994).
[12] L. Bürgi, O. Jeandupeux, A. Hirstein, H. Brune, and K. Kern, Phys. Rev. Lett. **81**, 5370 (1998).
[13] S. Crampin, H. Jensen, J. Kröger, L. Limot, and R. Berndt, Phys. Rev. B **72**, 035443 (2005).
[14] G. Hörmandinger and J. B. Pendry, Phys. Rev. B **50**, 18607 (1994).
[15] A. Bendounan, H. Cercellier, Y. Fagot-Revurat, B. Kierren, V. Yu. Yurov, and D. Malterre, Phys. Rev. B **67**, 165412 (2003).
[16] D. Malterre, B. Kierren, Y. Fagot-Revurat, S. Pons, A. Tejeda, C. Didiot, H. Cercellier, and A. Bendounan, New J. Phys. **88**, 391 (2007).
[17] J. Li, W. -D. Schneider, S. Crampin, and R. Berndt, Surf. Sci. **422**, 95 (1999).
[18] G. Grimvall, in *The Electron-Phonon Interaction in Metals, Selected Topics in Solid State Physics*, edited by E. Wohlfarth (North-Holland, New York, 1981).
[19] T. Valla, A. V. Fedorov, P. D. Johnson, and S. L. Hulbert, Phys. Rev. Lett. **83**, 2085 (1999).
[20] A. Eiguren, B. Hellsing, F. Reinert, G. Nicolay, E. V. Chulkov, V. M. Silkin, S. Hüfner, and P. M. Echenique, Phys. Rev. Lett. **88**, 066805 (2002).
[21] J. Kröger, L. Limot, H. Jensen, R. Berndt, S. Crampin, and E. Pehlke, Prog. Surf. Sci. **80**, 26 (2005).
[22] M. Becker, S. Crampin, and R. Berndt, Appl. Phys. A **88**, 555 (2007).
[23] J. Kliewer, R. Berndt, E. V. Chulkov, V. M. Silkin, P. M. Echenique, and S. Crampin, Science **288**, 1399 (2000).
[24] L. Vitali, P. Wahl, M. A. Schneider, K. Kern, V. M. Silkin, E. V. Chulkov, and P. M. Echenique, Surf. Science **523**, L47 (2003).
[25] T. Uchihashi, K. Kobayashi, and T. Nakayama, Phys. Rev. B **82**, 113413 (2010).